

Effects of Milling Methods on Tensile Properties of Polypropylene / Oil Palm Mesocarp Fibre Biocomposite

Nordin, N. I. A. A.^{1,2}, Ariffin, H.^{1,3*}, Hassan, M. A.1, Ibrahim, N. A.⁴, Shirai, Y.⁵ and Andou, Y.⁵

¹Department of Bioprocess Technology, Faculty of Biotechnology and Biomolecular Sciences, Universiti Putra Malaysia, 43400 Serdang, Selangor, Malaysia

²Faculty of Chemical and Natural Resources Engineering, Universiti Malaysia Pahang, Lebuhraya Tun Razak, 26300 Kuantan, Pahang, Malaysia

³Laboratory of Biopolymer and Derivatives, Institute of Tropical Forestry and Forest Products, Universiti Putra Malaysia, 43400 Serdang, Selangor, Malaysia

⁴Department of Chemistry, Faculty of Science, Universiti Putra Malaysia, 43400 Serdang, Selangor, Malaysia

⁵Graduate School of Life Science and System Engineering, Kyushu Institute of Technology, 2-4 Hibikino, Wakamatsu, Fukuoka 808-0196 Japan

ABSTRACT

The objective of this study was to evaluate the effects of milling methods on tensile properties of polypropylene (PP) / oil palm mesocarp fibre (OPMF) biocomposites. Two types of mills were used; Wiley mill (WM) and disc mill (DM). Ground OPMF from each milling process was examined for its particle size distribution and aspect ratio by sieve and microscopic analyses, respectively. Results showed that DM-OPMF had smaller diameter fibre with uniform particle size compared to the WM-OPMF. Surface morphology study by SEM showed that DM-OPMF had rougher surface compared to WM-OPMF. Furthermore, it was found that PP/DM-OPMF biocomposite had higher tensile strength compared to PP/WM-OPMF, with almost two-fold. Thus, it is suggested that small diameter and uniform size fibre may improve stress transfer and surface contact between the fibre and polymer matrix and cause well-dispersion of filler throughout the polymer resulted in better tensile strength of PP/DM-OPMF compared

to PP/WM-OPMF biocomposite. Overall, it can be concluded that disc milling could serve as a simple and effective grinding method for improving the tensile properties of biocomposite.

Keywords: Biocomposite, disc mill, oil palm mesocarp fiber, polypropylene, tensile properties, Wiley mill.

Article history:

Received: 19 May 2014

Accepted: 5 August 2014

E-mail addresses:

idamalina@yahoo.com (Nordin, N. I. A. A.),

hidayah@upm.edu.my (Ariffin, H.),

alihak@upm.edu.my (Hassan, M. A.),

alihak@upm.edu.my (Ibrahim, N. A.),

alihak@upm.edu.my (Shirai, Y.),

alihak@upm.edu.my (Andou, Y.)

*Corresponding Author

INTRODUCTION

Malaysia is the largest producer of palm oil contributing to 46% of the total world palm oil supply (MPOC, 2010). From the palm oil industries, about 77 million tonnes (dry weight) of biomass are generated annually consisting of 45 million tonnes of frond, 7 million tonnes of empty fruit bunch (EFB), 14 million tonnes of trunk and 11 million tonnes of mesocarp fibre (Ng *et al.*, 2010). Research has shown that oil palm biomass, especially EFB, has potential for biocomposite production (Khalid *et al.*, 2008; Rozman *et al.*, 2003). However, studies by Phattaraporn *et al.* (2011) and Thawien (2009) showed that oil palm mesocarp fiber (OPMF) also appeared to hold great potential in biocomposite industries, despite of less attention being given for effective utilization of OPMF. Currently, OPMF is treated as a waste product, which is burnt as fuel boiler inside the palm oil mill and as soil mulching in the plantation.

Grinding process is crucial in biocomposite production, especially if the biocomposite is to be prepared by compounding using internal mixer or extruder. This is done to allow a better wetting to the filler during processing. Shinoj *et al.* (2011) reported that a better interaction between fibre particles and polymer matrix could improve mechanical properties of the biocomposites. Mechanical properties of biocomposite reinforced by short lignocellulosic fibres can be contributed by several factors such as fibre particle size, aspect ratio and fibre/matrix adhesion. Fibre with high aspect ratio, i.e. long fibre with small diameter will give a higher surface area and hence, provide a larger contact area for the interaction of fibre particles and polymer matrix. High aspect ratio fibres bind better to the polymer compared to thick and short fibres. A typical sized fibre used for making biocomposite is less than 500 μm (Siyamak *et al.*, 2012; Bledzki & Faruk, 2006; Mikushina *et al.*, 2002).

Grinding is a common unit process to produce fine particles. Such fine particles are required for the utilization of natural lignocellulosic materials to enhance the accessibility of reactive agents (Bitra *et al.*, 2009) and to strengthen the interaction between different materials due to a higher surface area (Juliana *et al.*, 2012). There are different types of grinder with different fibre size reduction mechanisms, which result in different sizes of fibre particles. The common milling methods used are Wiley mill (WM) and disc mill (DM). Both the mills have different modes of action; WM is used to reduce the size of fibre by cutting, while disc milling involves a combination of actions which include compression, rubbing action, shearing and cutting.

As different mills may have different fibre breaking mechanisms, it is interesting to study the effects of fibre milling methods on the properties of the fibre and subsequently, its biocomposites. In this study, the effects of OPMF milling by WM and DM were investigated by evaluating the physical changes of OPMF in terms of particle size distribution, aspect ratio and morphological changes. Milled-OPMF obtained from both the milling techniques were then used for biocomposite preparation, while the effects of particle size distribution, aspect ratio and morphological surface on the tensile strength of the biocomposites were clarified.

MATERIALS AND METHODS

Raw Materials

OPMF was obtained from FELDA Serting Hilir Palm Oil Mill located in Negeri Sembilan, Malaysia. OPMF was disintegrated by manual washing and sorting. The OPMF was then sun dried. Samples were stored in sealed plastic bags at room temperature ($\pm 24^{\circ}\text{C}$) prior to further use. Polypropylene (PP) pellet (606251G112) was supplied by Polypropylene (Malaysia) Sdn. Bhd. and used as binding material.

Preparation of Oil Palm Mesocarp Fibre

Original OPMF used in this study had an average length of 20 – 30 mm. The size of OPMF was then reduced by using two different grinding methods. The first method involved the use of Wiley-type mill (Taiwan) Model CW-1 at the frequency of 50 Hz, with 5 rotating blades and a 0.5 mm screen. The second method used a disc mill (Ishiusu, Japan) Model RD 1-15, a stone type grinder with the gap between the stone fitted at the scale of 2 and operated in wet condition.

As for DM, the samples were wetted with distilled water at the ratio of 1:9 (fiber: water) in order to assist the disc-milling process. OPMF was pretreated by using the DM for 10 cycles. This was to ensure that only certain sizes of the fibre would be able to pass through the gap between the discs. After milling, DM-OPMF in slurry form (Fig.1a) was dried in an oven at 60°C to become a solid cake (Fig.1b). Dried solid cake was then crushed using stainless steels Waring blender to powderize the solid cake.

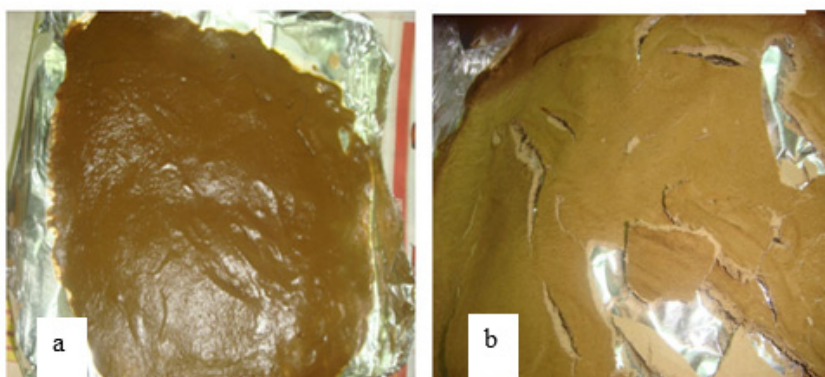


Fig.1: (a) DM-OPMF in slurry form; (b) Oven-dried DM-OPMF in the form of solid cake

Fabrication of the PP/OPMF Biocomposites

Only fibres that passed through 150 μm mesh size were used as biocomposite filler. Prior to blending, milled-OPMF were kept in an oven at 50°C for 24 h. The blending of PP with WM-OPMF and DM-OPMF was carried out using twin screw internal mixer model Haake Rheomix Polydrive at 170°C and 50 rpm rotor speed for 10 min. The biocomposites were prepared at 20 and 50% (w/w) of WM-OPMF and DM-OPMF based on weight ratio.

Characterization

Particle Size Analysis

Particle size distribution (PSD) of ground OPMF was determined by sieve analysis. The sample was divided into fractions with different particle sizes by sieving it. Ground WM- and DM-OPMF were sieved using a vibrating screener to pass through various mesh sizes of 150, 125, 100 and 75 μm for 20 min. The sieved samples were then weighed and subjected to particle size distribution. The percentage of PSD was calculated using equation 1 below.

$$\text{PSD (\%)} = \frac{\text{Weight of fraction (g)}}{\text{Weight of initial sample (g)}} \times 100\% \quad [1]$$

After sieving, WM-OPMF and DM-OPMF which passed through mesh size of 150 μm were analyzed by using microscope to observe their particle size geometry (length and diameter), followed by aspect ratio determination (length: diameter). A light microscope (Motic: Model BA310, China) provided with an image analyzer (Motic Images plus 2.0) was used to measure the length and diameter of the fibre particles.

Thermogravimetric Analysis of OPMF

Thermogravimetric analysis (TGA) was conducted on a TG analyzer model EXSTAR6000 TG/DTA6200 in order to confirm the compositional change of ground OPMF. OPMF powder sample (6 – 8 mg) was placed on an aluminium pan. The sample was heated from 50 – 550°C at a heating rate of 10°C/min under a nitrogen flow of 100 ml/min. The corresponding weight loss (μg) and its derivative, DTG ($\mu\text{g}/\text{min}$), were recorded.

Morphological Characterization

Surface morphology of WM-OPMF and DM-OPMF samples was observed under a scanning electron microscopy (SEM, model LEO 1455 VPSEM with Oxford Inca EDX). For the SEM analysis, oven-dried samples were mounted on the stub and gold-coated for 180 sec prior to the SEM observation. The SEM micrographs were obtained with an acceleration voltage of 20 kV.

Tensile Test of PP/OPMF Biocomposite

PP/OPMF blends were moulded in a mould with the dimension of 10 x 8 cm and a thickness of 1 mm. The PP/OPMF biocomposite was compressed with electrically heated platen pressed at 170°C at a pressure of 110 kg/cm² before it was cooled for 5 min at 50°C. The biocomposite sheet was cut into dumb-bell shape following the ASTM method D-638 type-V. Tensile test was carried out using Instron Universal Testing Machine (Model 4302 Series IX) based on ASTM D638. The test was conducted at a constant crosshead speed of 5 mm/min, load cell of 1 kN and a gauge length of 10 mm. An average of five readings was taken as the resultant value.

RESULTS AND DISCUSSION

Particle Size Analysis

PSD of WM-OPMF and DM-OPMF is shown in Fig.2. DM-OPMF showed a higher percentage of small sized particles ($<75 \mu\text{m}$) compared to WM-OPMF by almost three folds. From the same figure, it can be seen that disc milling was able to reduce the diameter of OPMF, with more than 50% of the OPMF had a particle size of $<100 \mu\text{m}$. This is in contrary with WM, whereby only 20% of the fibres had a particle size of $<100 \mu\text{m}$. This observation was contributed by the mode of action of each milling process, whereby WM was only able to shorten the length of the OPMF by cutting knife/teeth without affecting the diameter of the fibre. On the other hand, DM reduced the size of OPMF by milling between the rotating disc resulting cutting to short length, imparting and shearing to a smaller diameter and exposing microfibrils of the OPMF. From the physical appearance of the OPMF powder with size $<150 \mu\text{m}$, it can be observed that DM-OPMF had finer powder compared to WM-OPMF (see Fig.3). This observation is in agreement with the result shown in Fig.2.

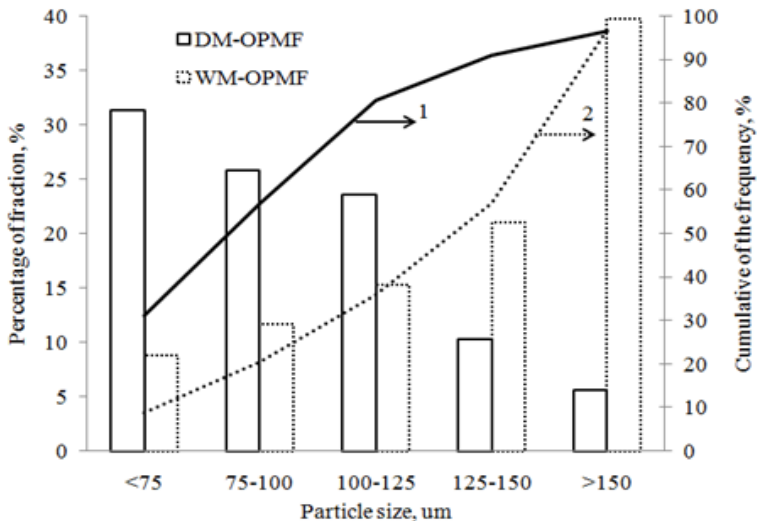


Fig.2: Particle size distribution of DM-OPMF and WM-OPMF. Bar graphs indicate fraction of particle size of the fibre (%) and lines show cumulative of the fraction (%) for, (1) DM-OPMF and (2) WM-OPMF.

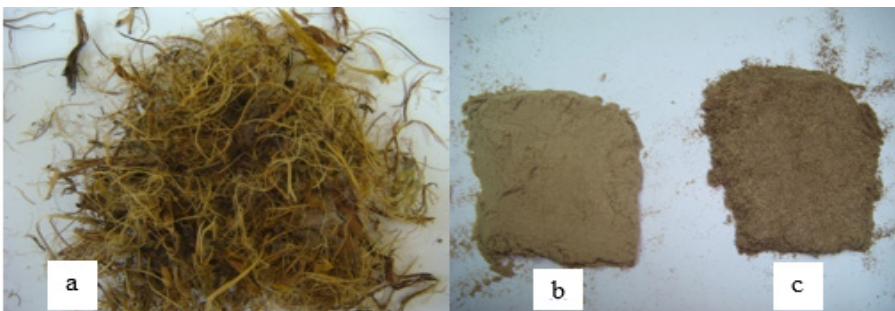


Fig.3: Physical appearance of: (a) raw OPMF; (b) powdered DM-OPMF; (c) ground WM-OPMF; after sieving to pass mesh size of $150 \mu\text{m}$.

Ground fibres were also measured for their length, L and diameter, D by microscopic analysis. The distribution of the L and D of the milled-OPMF is shown in Fig.4. A small diameter fibre indicates that the cellulose macrofibrils have been ripped into microfibrils due to mechanical action. Overall, it is seen that both L and D of the DM-OPMF converged towards the lower size with average L and D values of <200 and <50 μm , respectively. WM-OPMF, on the other hand, had a wider distribution of fibre L and D. This observation contributes to the aspect ratio values of DM-OPMF and WM-OPMF (Fig.5). Since DM-OPMF had low L and D values, this contributed to the low aspect ratio of DM-OPMF, with an average aspect ratio of 5. Even though WM-OPMF seemed to have high aspect ratio with average value of ≈ 10 , the average length and diameter of the fibres are relatively high for biocomposite preparation (Montano-Leyva *et al.*, 2013). Juliana *et al.* (2012) discussed that thin and long particles might increase the contact area between the fibres and polymer matrix, resulting in a better adhesion of the two materials. In this study, disc milling was used to get thin fibres. Overall, the particle size of disc milled-OPMF is much smaller compared to that obtained from Wiley mill.

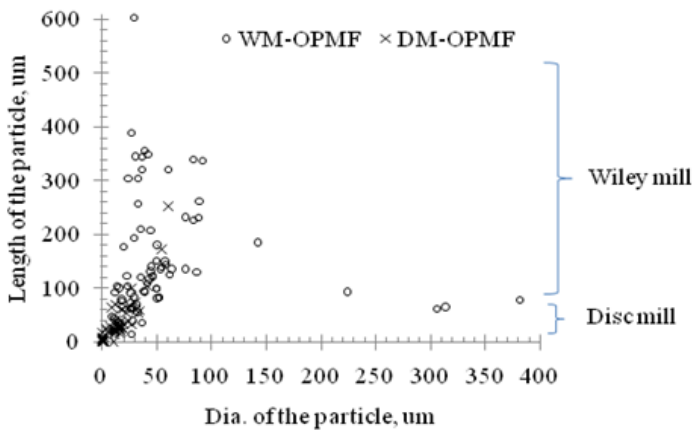


Fig.4: Distribution of diameter and length of DM-OPMF and WM-OPMF particles

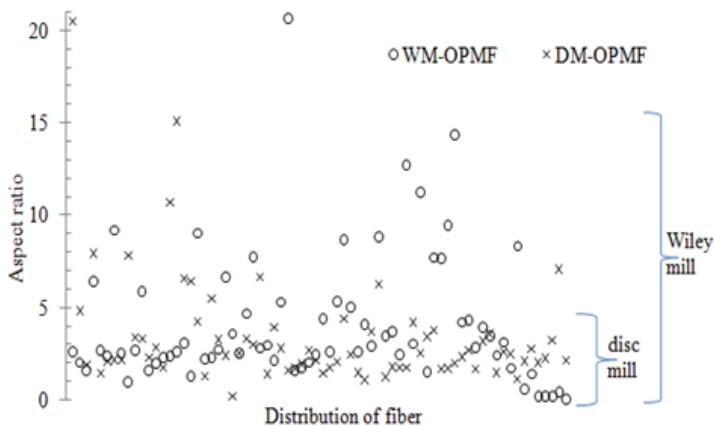


Fig.5: Distribution of the aspect ratio of DM-OPMF and WM-OPMF

Morphological Analysis

SEM analysis was done to support the above findings, as shown in Figures 6a–e. Fig.6a shows the SEM micrograph of original OPMF fibre (not ground), whereby it can be observed that silica bodies are deposited on the entire of fibre surface. Similar observations were also reported by Chua *et al.* (2009) and Nik Mahmud *et al.* (2013). Figures 6b–e show the SEM micrographs of DM- and WM-OPMF. Overall, it is shown that DM-OPMF had smaller fibre size (Fig.6c) compared to WM-OPMF (Fig.6e). This observation can be explained by the mode of action of disc milling which involves crushing, shearing and cutting of the fibre samples (Vishwanathan *et al.*, 2011). The microfibrillated structure of DM-OPMF can be clearly observed at a higher magnification (see Fig.6b). The shearing force by rotating disc of DM was able to open the pores of the fibre, causing PP to penetrate within the OPMF fibrils easily.

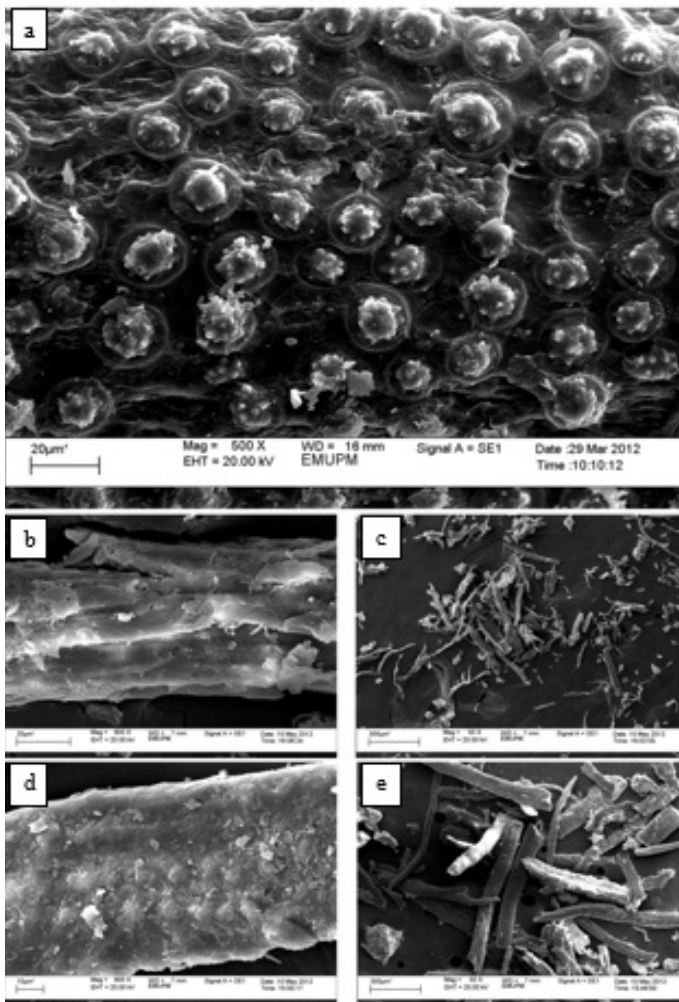


Fig.6: The SEM micrographs of OPMF: (a) original OPMF (not ground); (b) DM-OPMF (800x magnification) (c); DM-OPMF (50x magnification) (d) WM-OPMF (800x magnification), and (e) WM-OPMF (50x magnification). Silica bodies were found deposited on the surface of original OPMF fibre

It is interesting to observe that silica bodies were removed from the surface of milled-OPMF. Both DM- and WM-OPMF showed no silica bodies on their surface. According to Shinoj *et al.* (2011), removal of silica bodies could create perforated silica craters, which would result in a better fibre-matrix interfacial adhesion. This can be explained by the creation of rougher fibre surface which is more advantageous in helping the penetration of melt polymer into the fibre (Shinoj *et al.*, 2010).

Thermal Stability of DM-OPMF and WM-OPMF

Thermal analysis of the milled fibres was done to evaluate the thermal stability of the samples. Fig.7 shows TG and DTG curves of DM-OPMF and WM-OPMF. From the TG curves, both DM-OPMF and WM-OPMF had almost similar thermal degradation trend with three-step degradation indicating the three major components in lignocellulose; hemicellulose, cellulose and lignin. Incomplete decomposition at 550°C indicates that some lignin fractions were degraded at a higher temperature range (Yang *et al.*, 2007). On the other hand, DTG curves showed two apparent peaks at the temperature range of 250–320°C and 320–390°C, indicating the degradation of hemicellulose and cellulose, respectively.

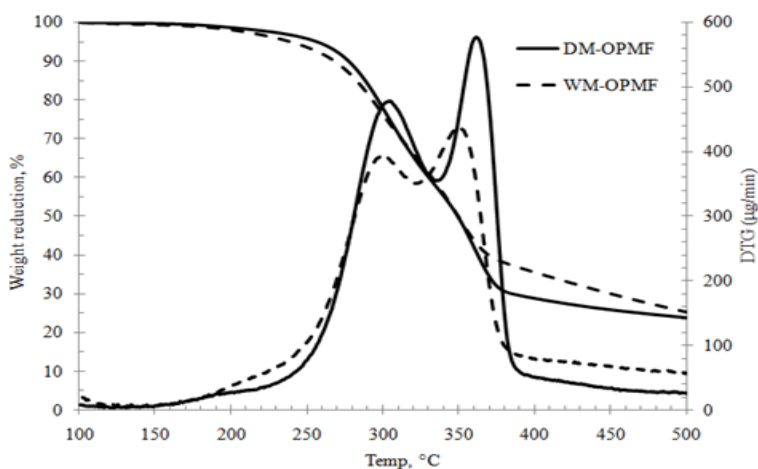


Fig.7: TG and DTG curves of DM-OPMF and WM-OPMF

TABLE 1: Summary of degradation temperature at 5, 20 and 50% obtained by TGA of DM-OPMF and WM-OPMF

Sample	T _{5%} (°C)	T _{20%} (°C)	T _{50%} (°C)	T _p (°C)	Weight loss (%)		Residue at 550 °C (%)
					Temp region (°C)		
					150-250	300-450	
DM-OPMF	256.5	296.6	349.0	299.7, 359.3	4	52	23
WM-OPMF	238.8	292.8	349.2	295.4, 346.6	7	46	24

T_{n%} represents the onset decomposition temperature of 5, 20 and 50% weight loss, T_p represents peak temperature of DTG.

A summary of the thermal decomposition profile of each sample is presented in Table 1. The results of decomposition temperature at different weight losses (5%, 20% and 50%), the onset temperature of TGA and peak temperature of DTG are tabulated. From the results, it is seen that DM-OPMF had higher thermal stability compared to WM-OPMF. For example, T5% of DM-OPMF was recorded at a higher temperature (256.5°C) compared to that of WM-OPMF (238.8°C). This indicates that some components in WM-OPMF degraded at a lower temperature. Lignin has been reported to have a wide thermal degradation temperature range between 150 – 900°C (Yang *et al.*, 2007; Bachtiar *et al.*, 2013). Therefore, based on the weight loss at the low temperature as shown in TG results, it is suggested that some lignin fractions were removed during disc-milling, causing the thermal stability of DM-OPMF to improve. This is supported by the residual weight of OPMF at 370°C onwards, which showed that DM-OPMF had lower residual weight compared to WM-OPMF. This indicates that lignin content in DM-OPMF was lower as compared to WM-OPMF.

Lignin loss during disc-milling can be explained by shear effect during disc-milling. It is suggested that the shear and friction during disc milling disrupted lignocellulosic structure, as proven by the formation of microfibrillated structure. This is supported by Fig.4 which shows that DM-OPMF has a smaller fibre diameter ($\sim <50 \mu\text{m}$) compared to that of WM-OPMF (up to $400 \mu\text{m}$). In lignocellulose material, lignin acts as glue in between the cellulose fibrils (Reddy & Yang, 2005) causing them to arrange tightly in stacks and hence giving strength to the material. The disruption of lignin causes the cellulose fibrils to tear apart and form microfibrils. Moreover, Mikushina *et al.* (2002) highlighted that milling is expected to cause chemical changes in lignin. Additionally, the presence of lignin in fibre sample is usually shown by the dark appearance of the fibre. Herewith, it is shown in Fig.3 (b) and (c) that DM-OPMF had lighter colour compared to that of WM-OPMF.

Thermal and Tensile Properties of OPMF/PP Biocomposite

DM-OPMF and WM-OPMF fibres in the particle size of $<150 \mu\text{m}$ were blended with PP in the mixer at 20 and 50% (w/w) of fibre loading. PP/OPMF biocomposites were tested for their thermal stability and tensile strength.

Generally, PP has higher thermal stability compared to lignocellulose, while the biocomposite samples had better thermal stability compared to OPMF alone, as seen in Figures 7 and 8. Bachtiar *et al.* (2013) described the degradation temperature for biocomposite to commonly fall between the degradation temperature of polymer matrix and the filler. From the results obtained, the biocomposites prepared from DM-OPMF and WM-OPMF at 20 and 50% (w/w) of fibre loading showed almost similar trend in thermal degradation from the beginning to completion, indicating that alteration in lignin content in DM-OPMF did not really affect the biocomposite thermal property. Fig.8 shows the TG and derivative TG (DTG) curves of DM- and WM-OPMF biocomposite at 50% (w/w) of fibre loading. From the DTG curve in Fig.8, three maximum peaks can be observed. The first peak temperature for DM- and WM-OPMF biocomposite was the same at 292°C. This peak indicated hemicelluloses decomposition as reported by Yang *et al.* (2007); degradation temperature of hemicelluloses ranged from 220 to 318°C. The second peak was degradation of cellulose that could be observed at 359°C

for DM-OPMF which was slightly higher than WM-OPMF at 356°C. Polypropylene in the biocomposite was decomposed at the peak temperature of 473 and 471°C for DM- and WM-OPMF, respectively.

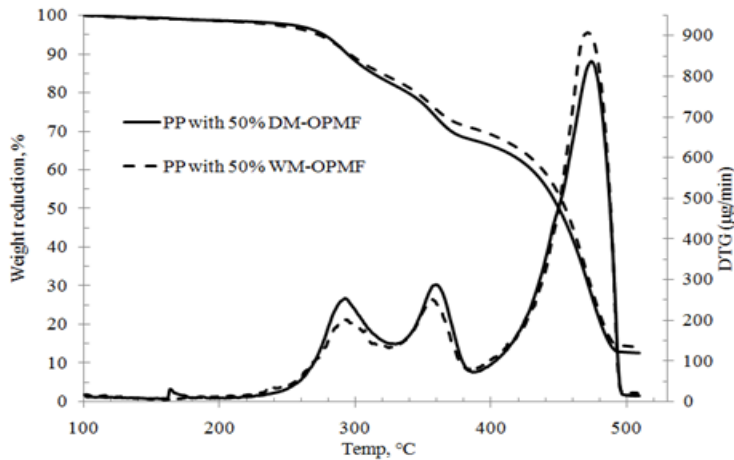


Fig.8: The TG and DTG curves of PP/DM-OPMF and PP/WM-OPMF biocomposites

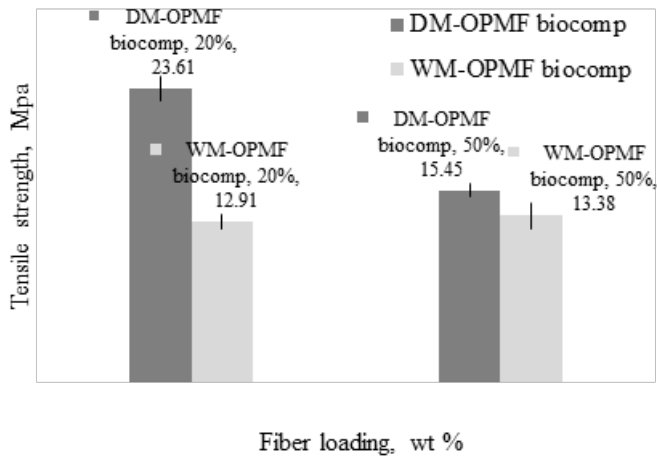


Fig.9: Tensile strength of DM-OPMF and WM-OPMF biocomposites prepared from fibre with particle size <150 µm with 20 and 50 % (w/w) fibre loading

The tensile strength of WM-OPMF and DM-OPMF biocomposites were tested in order to evaluate the performance of the biocomposites. Fig.9 shows the tensile strength of PP/WM-OPMF and PP/DM-OPMF biocomposites at 20 and 50% (w/w) fibres loading. There were marked differences in the tensile strength value for biocomposite prepared from DM-OPMF with that of WM-OPMF, especially for the sample with 20% (w/w) of fibre loading. Biocomposite with 20% (w/w) DM-OPMF had a tensile strength of 23.6 MPa, which is 83% stronger compared to the biocomposite with 20% (w/w) WM-OPMF. The same observation could be seen for the biocomposite prepared with 50% (w/w) fibres, even though the difference

in the tensile strength value was not as high as that for the biocomposite with 20% (w/w) fibres. The higher tensile strength demonstrated by the biocomposite prepared from DM-OPMF could be contributed by the smaller size of the fibre particles depicted in Figures 2, 4 and 6. Even though the OPMF used in this study were obtained after sieving to pass through 150 μm mesh, the microscopic analyses by light microscope and SEM revealed that the fibres with larger particle size (long fibres) could still pass through the mesh since the fibres passed through the mesh vertically. Based on the observation, it can be concluded that DM-OPMF had smaller fibre size compared to WM-OPMF and hence, it gave a higher surface area per volume which then improved the surface contact between fibres and polymer matrix. The higher surface contact between fibres and polymer improved the physical adhesion between the two materials. This explained why PP/DM-OPMF had a better tensile strength compared to PP/WM-OPMF. Moreover, the small size of DM-OPMF might have improved the stress transfer between polymer matrix and fibres compared to longer fibres. Fibres with small diameter also cause them to be arranged in the polymer matrix easily, leading the tensile strength to be improved in the PP/DM-OPMF biocomposite.

CONCLUSION

Two different grinding techniques were used to grind OPMF for biocomposite production. DM-OPMF showed a higher percentage of small sized particles ($<75 \mu\text{m}$) compared to WM-OPMF by almost three folds. Disc milling was able to disrupt lignin structure and hence unmasked the macrofibrils to form microfibrils. This eventually affected the tensile strength of PP/OPMF biocomposites. PP/DM-OPMF biocomposite with 20% (w/w) fibres had a tensile strength of 23.6 MPa, which is 83% higher compared to the PP/WM-OPMF biocomposite. This study revealed that the milling method has pronounced effects in improving the mechanical property of biocomposites. Overall, disc milling yielded smaller sized fibre particles compared to Wiley mill and hence, enhanced the surface contact between fibres and polymer matrix.

ACKNOWLEDGEMENTS

The authors would like to thank Professor Dr Haruo Nishida from Kyushu Institute of Technology (Kyutech), Japan, for allowing them to use the TG analyzer in his lab, and to Mr. Ahmad Muhaimin from Universiti Putra Malaysia (UPM) for assisting them with the wet disc mill. The authors are grateful for the provision of scholarship from the Ministry of Higher Education (MOHE) to the first author.

REFERENCES

- Bachtiar, D., Sapuan, S. M., Zainudin, E. S., Khalina, A., & Dahlan, K. Z. H. M. (2013). Thermal properties of alkali-treated sugar palm fibre reinforced high impact polystyrene composites. *Pertanika Journal Science & Technology*, 21, 141–150.
- Bitra, V. S. P., Womac, A. R., Chevanan, N., Miu, P. I., Igathinathane, C., Sokhansanj, S., & Smith, D. R. (2009). Direct mechanical energy measures of hammer mill comminution of switchgrass, wheat straw, and corn stover and analysis of their particle size distributions. *Powder Technology*, 193, 32–45.

- Bledzki, A. K. & Faruk, O. (2006). Microcellular injection molded wood fiber-PP composites: part II – Effect of wood fiber length and content on cell morphology and physico-mechanical properties. *Journal of Cellular Plastics*, 42, 77–88.
- Chua, S. C., Tan, C. P., Mirhosseini, H., Lai, O. M., Kamariah, L., & Baharin, B. S. (2009). Optimization of ultrasound extraction condition of phospholipids from palm-pressed fiber. *Journal of Food Engineering*, 92, 403–409.
- Juliana, A.H., Paridah, M.T., Rahim, S., Nor Azowa I., & Anwar U.M.K. (2012). Properties of particleboard made from kenaf (*Hibiscus cannabinus* L.) as function of particle geometry. *Materials and Design*, 34, 406–411.
- Khalid, M., Ratnam, C. T., Chuah, T. G., Ali, S., & Choong, T. S. Y. (2008). Comparative study of polypropylene composites reinforced with oil palm empty fruit bunch fiber and oil palm derived cellulose. *Materials & Design*, 29, 173–178.
- Mikushina, I. V., Troitskaya, I. B., Dushkin, A. V., & Bazarnova, N. G. (2002). Changes in the chemical composition of wood during mechanochemical treatment. *Chemistry for Sustainable Development*, 10, 441–445.
- Montano-Leyva, B., Silva, G. G. D., Gastaldi, E., Torres-Chavez, P., Gontarda, N., & Angellier-Coussy, H. (2013). Biocomposites from wheat proteins and fibers: Structure/mechanical properties relationships. *Industrial Crops and Products*, 43, 545–555.
- Ng, F., Yew, F., Basiron, Y., & Sundram, K. (2010). A renewable future driven with Malaysian palm oil-based green technology. *Journal of Oil Palm & the Environment*, 2, 1–7.
- Nik Mahmud, N. A., Baharuddin, A. S., Bahrin, E. K., Sulaiman, A., Naim, M. N., & Zakaria, R. (2013). Enzymatic saccharification of oil palm mesocarp fiber (OPMF) treated with superheated steam. *BioResources*, 8, 1320–1331.
- Phattaraporn, T., Waranyou, S., & Thawien, W. (2011). Effect of palm pressed fiber (PPF) surface treatment on the properties of rice starch films. *International Food Research Journal*, 18, 287–302.
- Reddy, N. & Yang, Y. (2005). Biofibers from agricultural byproducts for industrial applications. *TRENDS in Biotechnology*, 23(1).
- Rozman, H. D., Saad, M. J., & Ishak, Z. A. M. (2003). Flexural and impact properties of oil palm empty fruit bunch (EFB)-polypropylene composites-the effect of maleic anhydride chemical modification of EFB. *Polymer Testing*, 22, 335–341.
- Shinoj, S., Visvanathan, R., & Panigrahi, S. (2010). Towards industrial utilization of oil palm fibre: Physical and dielectric characterization of linear low density polyethylene composites and comparison with other fibre sources. *Biosystems Engineering*, 106, 378–388.
- Shinoj, S., Visvanathan, R., Panigrahi, S., & Kochubabu, M. (2011). Oil palm fiber (OPF) and its composites: A review. *Industrial Crops and Products*, 33, 7–22.
- Siyamak, S., Ibrahim N. A., Abdolmohammadi, S., Yunus, W. M. Z. W., & Rahman, M. Z. AB. (2012). Enhancement of mechanical and thermal properties of oil palm empty fruit bunch fiber poly (butylene adipate-co-terephthalate) biocomposites by matrix esterification using succinic anhydride. *Molecules*, 17, 1969–1991.
- Thawien, W. (2009). Microcomposites of rice starch film reinforced with microcrystalline cellulose from palm pressed fiber. *International Food Research Journal*, 16, 493–500.

Vishwanathan, K.H., Singh, V., & Subramanian, R. (2011). Wet grinding characteristics of soybean for soymilk extraction. *Journal of Food Engineering*, 106, 28–34.

Yang, H., Yan, R., Chen, H., Lee, D. H., & Zheng, C. (2007). Characteristics of hemicellulose, cellulose and lignin pyrolysis. *Fuel*, 86, 1781–1788.